Fine structure of the metastable a 3 Σ u + state of the helium molecule

W. Lichten, M. V. McCusker, and T. L. Vierima

Citation: The Journal of Chemical Physics **61**, 2200 (1974); doi: 10.1063/1.1682292
View online: http://dx.doi.org/10.1063/1.1682292
View Table of Contents: http://scitation.aip.org/content/aip/journal/jcp/61/6?ver=pdfcov
Published by the AIP Publishing

Fine structure of the metastable $a\,^3\Sigma_u^+$ state of the helium molecule*

W. Lichten, M. V. McCusker, and T. L. Vierima

Yale University, New Haven, Connecticut 06520
(Received 9 April 1974)

We have measured the spin–spin, electronic fine structure of the $a\,^3\Sigma_u^+$ metastable state of He_2 by means of a molecular beam, magnetic resonance apparatus, with the flowing afterglow of a pulsed, helium discharge as the source. The zero field separations in the $N=1$ and $N=3$ rotational levels, probably in the $v=0$ vibrational state, are (in MHz) $N=1$: $J=0\leftrightarrow J=1$:2199.968 ± 0.01, $J=1\leftrightarrow J=2$: 873.668 ± 0.007; $N=3$: $J=2\leftrightarrow J=3$: 1323.911±0.006, $J=3\leftrightarrow J=4$: 964.992±0.006, where the errors quoted are three standard deviations of the mean. From these measurements and from a separate determination of the level order, the interaction constants for these states are the following (in MHz): spin–spin: λ:−1098.773 $\pm$0.005($N=1$), −1096.803$\pm$0.004($N=3$), spin–rotation: γ: −2.421$\pm$0.003($N=1$), −2.414$\pm$0.001($N=3$), where the errors are 3σ.

I. INTRODUCTION

Helium, the noblest of all atoms, forms no chemical compounds with itself or any other atoms. Unlike other atoms, it cannot even form a stably bound Van der Waals molecule with itself.[1] Ever since the discovery of the helium band spectrum by Curtis and Goldstein[2] in 1913, it has been known that stably bound, excited states of He_2 exist.[3] In particular, Phelps[4] and, subsequently, many others[5–11] have detected optical absorption in gas and liquid phases of the helium molecule in the metastable $a^3\Sigma_u^+$ state. The demonstrated existence of a long-lived paramagnetic state has raised the possibility of a precision measurement of the fine structure (fs) in one of the simplest molecules in nature. An effort to make this measurement in liquid helium by Hill *et al.* was reported,[7] but no resonances were observed.[12] In this paper, we report such a measurement by means of the molecular beam, magnetic resonance (Rabi) technique.

Some time ago, one of us gave a historical summary of previous work on molecular fs and related fields.[13] We begin this article by bringing that account up to date.

A. History of previous observations

1. Simple atomic systems

The precise agreement between experiment and theory for electromagnetic properties of simple atomic systems has been made even more complete over the past decade. The value of the fs constant $\alpha=1/137.03602(21)$,[14] which lies at the heart of any calculation of fs, recently has been based entirely on the hfs of H and the A. C. Josephson effect in superconducting solids.[14] Measurements of properties of simple, one-electron systems are now in essentially good agreement with theory with no outstanding discrepancies.[15] Likewise, great progress has been made with two-electron systems.[15] In particular, theory and experiment[16,17] agree to within a few parts per million for the fs of He $(1s, 2p)^3P_{2,1,0}$. This agreement was achieved by solving the difficult problem of computing small second order terms involving other electronic states. This problem becomes more difficult in interpretation of molecular fs, as we shall show.

2. Molecular systems

It is of interest to make a comparison among the fs investigations of three simple molecules, H_2^+, H_2, and He_2. In H_2^+, studied by an optical pumping technique by Jefferts,[18] the $^2\Sigma_g^+$ ground state has a single electron which has no orbital angular momentum. Thus the only interactions present are the spin–rotation, magnetic contact, and dipolar hfs and a very weak interaction of nuclear spin with rotation.

In the one-electron, molecular system of H_2^+ $^2\Sigma_g^+$, excellent agreement (~1%) between experiment[18] and theory[19,20] exists. In these calculations, second-order contributions of other electronic states are very small.[20]

In H_2, $^3\Pi$ states[13,21–25] there are two unpaired electron spins, orbital angular momentum, and molecular rotation in parahydrogen; in orthohydrogen, there are also two unpaired nuclear spins. The electronic spin–spin, spin–orbit, and spin–other-orbit interactions are present, in addition to the terms already listed for H_2^+. Also, there are terms like the orbital–magnetic hfs interaction and orbital–rotation terms which add even more richness to the structure. These have been analyzed theoretically by many authors.[23]

In the case of the c and d $^3\Pi_u$ states of H_2, *ab initio* calculations by Lombardi[26] and Jette[27] agree with experimental measurements by Freund and Miller[24,25] and Brooks, Lichten and Reno and Vierima[21,22] to within a discrepancy of the order of 1% for the one-electron hfs operators and to ~2%–4% for the two-electron fs operators. No second-order terms involving other electronic states have been calculated. At present, there are no measurements of fs in $^3\Sigma$ states in H_2.

Mulliken and Monk[28] partially resolved the optical fs of the $b^3\Pi_g$ state of He_2. Despite further efforts by one of us, with resolving powers up to 600 000, no further progress has been made with this problem.[29] No visible splitting or even broadening has been observed in the optical spectra of any other state of He_2.

3. Spin–spin interactions in molecules

Molecules in $^3\Sigma$ states are of interest, because the first order fs is caused by magnetic, spin–spin interac-

tion between two electrons; spin–orbit interaction is absent in first order. The theory of this interaction was originated by Kramers,[30] improved by Schlapp,[31] and elaborated by many authors.[32–42] It is well known that second order spin–orbit interaction has the same form as spin–spin interaction.[32–36,38–42] Yet, despite more than forty years study of the $^3\Sigma_g^-$ ground state of O_2, the discrepancy between theory and experiment remains at 20% and a satisfactory solution still eludes the theorists.[42] (See Table IV.) In NH, where spin–orbit effects are smaller, theory and experiment agree within a few percent (see Table IV).[42b] Because the spin–orbit interaction in He_2 is orders of magnitude smaller than in O_2, the prospects for a more successful theoretical interpretation made this investigation seem promising to us. A more detailed description of this interpretation is given in the discussion of our results. (See Sec. III. B.)

B. The spectrum of molecular helium

The molecular spectrum of helium is one of the most thoroughly observed and analyzed in all of molecular spectroscopy.[3] More than 60 electronic states have been observed and analyzed.[3] It is of historical interest to note that the first experimental measurement of the spin of the He^3 nucleus was by Douglas and Herzberg, who analyzed the alternation of intensity in the band spectrum of He_2^3.[43] Recently, several theoretical and experimental papers have discussed the nature of the potential curves of He_2, which have an unusually large number of potential maxima.[44] (See Fig. 1.)

For some time after the discovery of the spectrum of He_2,[2] the absence of any vibrational structure in the bands remained a mystery. It is now known that the cause for this situation lies in the relative weakness of excitation of any excited vibrational levels in molecular helium.[45] A knowledge of the relative vibrational populations is very important for the interpretation of our experiment.

Since the early work of Curtis and Goldstein,[2] the most common technique for producing the molecular spectrum of helium has been to observe the afterglow of a discharge in helium at a pressure of a few centimeters of mercury. There have been many investigations of molecule formation in noble gas discharges, discharge afterglows,[4–6,10,11,46–56] and electron bombarded liquid helium[7–9]; these investigations have been stimulated by the recent development of the molecular xenon laser.[57] It is generally accepted that helium molecules are predominantly formed in a discharge by recombination of molecular ions; however, the details of the formation process are still controversial.[52–55]

C. The structure of molecular helium

The ground state of molecular helium He_2, $X^1\Sigma_g^+$ $(1s_A^2 1s_B^2 = \sigma_g 1s^2 \sigma_u 1s^2)$ consists of a closed shell, electronic wavefunction of four electrons filling the two lowest atomic orbitals $1s_A$ and $1s_B$, or equivalently, the two molecular orbitals (MO) $\sigma_g 1s$ $(1\sigma_g$ or $1s\sigma_g)$ and $\sigma_u 1s$

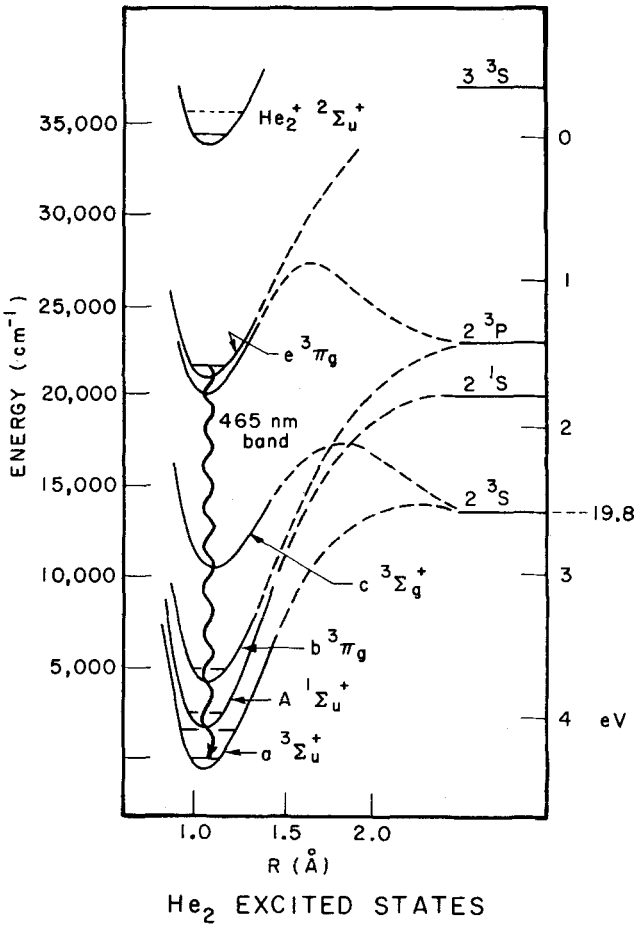

FIG. 1. Selected excited energy levels of the He_2 molecule. A cascade mechanism which populates the metastable $a^3\Sigma_u^+$ state is shown.

$(1\sigma_u$ or $2p\sigma_u)$. Each of these two MO's is approximately a linear combination of atomic orbitals (LCAO)

$$\sigma_g 1s \approx \frac{1s_A + 1s_B}{\sqrt{2}}; \quad \sigma_u 1s \approx \frac{1s_A - 1s_B}{\sqrt{2}}.$$

In singly excited states of He_2, in the vicinity of the equilibrium internuclear distance ($r_e \sim 1$ Å), the molecule consists of an $He_2^+(\sigma_g 1s)^2(\sigma_u 1s)$, $^2\Sigma_u^+$ core surrounded by an electron in a Rydberg MO. (See Figs. 1, 2.) The metastable $a^3\Sigma_u^+$ state, which is the object of the present study, has the electron configuration $(\sigma_g 1s)^2(\sigma_u 1s)(\sigma_g 2s)$. The $\sigma_g 2s$ MO can be approximated by a linear combination of $2s$ atomiclike orbitals centered on each of the two atoms. (See Fig. 2.)

The spins of the $\sigma_u 1s$ and $\sigma_g 2s$ electrons are unpaired, giving a triplet state with electronic spin angular momentum $S = 1$. The magnetic fine structure of this state arises from the dependence of the magnetic spin–spin interaction energy upon the spin vector orientation. (See Sec. III. B for a more detailed discussion.)

Since only the $X^1\Sigma_g^+$ ground state is below the $a^3\Sigma_u^+$ state and because the selection rule $\Delta S = 0$ is well obeyed in He_2, the a state is metastable. The lifetime of an isolated molecule is at least 100 msec.[4,8]

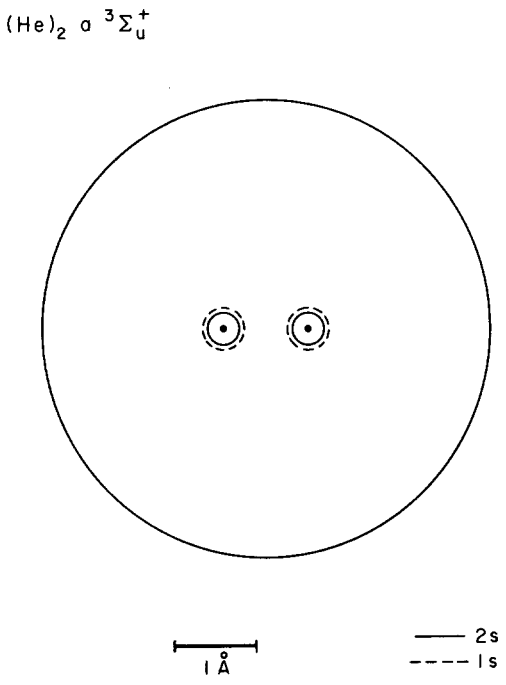

FIG. 2. Schematic diagram of the contours of maximum radial probability density of the orbitals of the He_2 molecule. Solid lines $\sigma_g 2s$. Broken lines $\sigma_g 1s$, $\sigma_u 1s$.

II. THE EXPERIMENTAL METHOD

A. Apparatus

At the beginning of this experiment, we considered the possibility of using optical pumping to produce polarized helium molecules for rf spectroscopy.[56] An alternative was to develop a metastable molecule source for the conventional molecular beams–magnetic resonance (MBMR) machine which has been in use in this laboratory to study the fine and hyperfine structure of metastable hydrogen molecules.[13,21,22] We chose the latter course of action, largely because of the greater convenience of existing equipment.

Because the helium molecule has a purely repulsive ground state, direct electron impact excitation[12,13,21,22,58] cannot be used to produce the metastable molecules. We have seen (Sec. I. B) that helium molecules can be formed in discharge tubes. A source, then, requires some adaptation of a discharge tube similar to those used in the traditional spectroscopy experiment.[2,45,59]

A discharge tube source of metastable (2^3S_1) helium atoms was successfully used in an MBMR machine by V. W. Hughes and co-workers.[60] They observed optimum performance at the lowest pressures at which they could operate (near 0.1 torr). No evidence of molecules was observed. Presumably, raising the pressure in such a discharge tube to a level high enough to ensure the production of molecules produced so high a pressure in the source chamber that the beam was destroyed by collisions.

We observed molecule production with the MBMR machine with the following arrangement (see Fig. 3): a 3 mm diameter hole was drilled in a pure aluminum cathode 1 cm thick; this was waxed onto the discharge tube and the axis of the hole was aligned with the MBMR machine. The gas from the discharge flowed through the hollow cathode and entered a chamber which was exhausted by a fast mechanical pump (Roots Blower, Stokes Model 1722, pumping speed for air = 600 l/s at 0.25 torr). A 0.3 cm×0.003 cm slit was placed on the wall of this region and defined the beam. A differentially pumped region separated this chamber from the magnet series and its vacuum pump. The pressure in the discharge tube was typically 10 torr; at the exit of the cathode, 0.13 torr; after the beam defining slit, 5×10^{-5} torr; and at the detector, 8×10^{-6} torr. Oil diffusion pumps without liquid N_2 trapping were used (see Fig. 3).

A pulsed high voltage discharge was used. A well regulated power supply (Fluke Model 415B) was used with a M.I.T. Model 9 modulator/driver unit; an additional winding was added to the output pulse transformer to double the output voltage. Typical electrical operating conditions were power supply voltage, 1750 V; pulse length, less than 1 μsec; repetition rate, 3–10 kHz; average power into the driver, 15 W (a very small fraction of this power was actually consumed in the discharge tube). Except for the pressure, which was somewhat low, these operating conditions were close to those needed to produce an optimally intense visible molecular helium spectrum in the discharge tube. We placed the cathode connection at the gas exit of the discharge. Reversal of the anode and cathode connections quenched both the visible and rf molecular helium spectrum, apparently through cataphoretic concentration of impurities in the discharge.

Molecules were best produced under conditions of rather high gas flow rate so that a bright afterglow could be seen outside the exit of the cathode. Visual observations of the discharge indicated that the interior of the cathode was brighter than the glow in the discharge tube or the afterglow. We consistently observed that the optimum atomic and molecular signal in our detector were obtained when the discharge conditions were adjusted so that there was a moderate afterglow. This subjective criterion was found to be quite reliable in setting up the apparatus each day. It was essential that the exit slit be placed well inside the visible afterglow. The final cathode-to-slit separation was approximately 1 cm. The entire discharge tube was moved relative to the exit slit to optimize the signal-to-noise ratio.[61]

The gas throughput in our experiment was ~16 torr l/s. The bulk flow velocity in the discharge tube, where the pressure is 10 torr, was $\sim 1.5\times10^3$ cm/sec. In the visible afterglow region at the exit of the cathode, the flow velocity was estimated to be 10^5 cm/sec. The bulk flow velocity in the exhaust tube near the pump, where the pressure was 0.03 torr, was approximately 3×10^4 cm/sec.

The MBMR machine used in this experiment was a modification of that used in previous experiments with metastable hydrogen molecules.[13,21,22] Molecules that passed through the A magnet were refocused by the B magnet onto a stop wire located in front of the detector. When a radio-frequency magnetic field of the appropriate frequency and intensity was applied to the hairpin in the

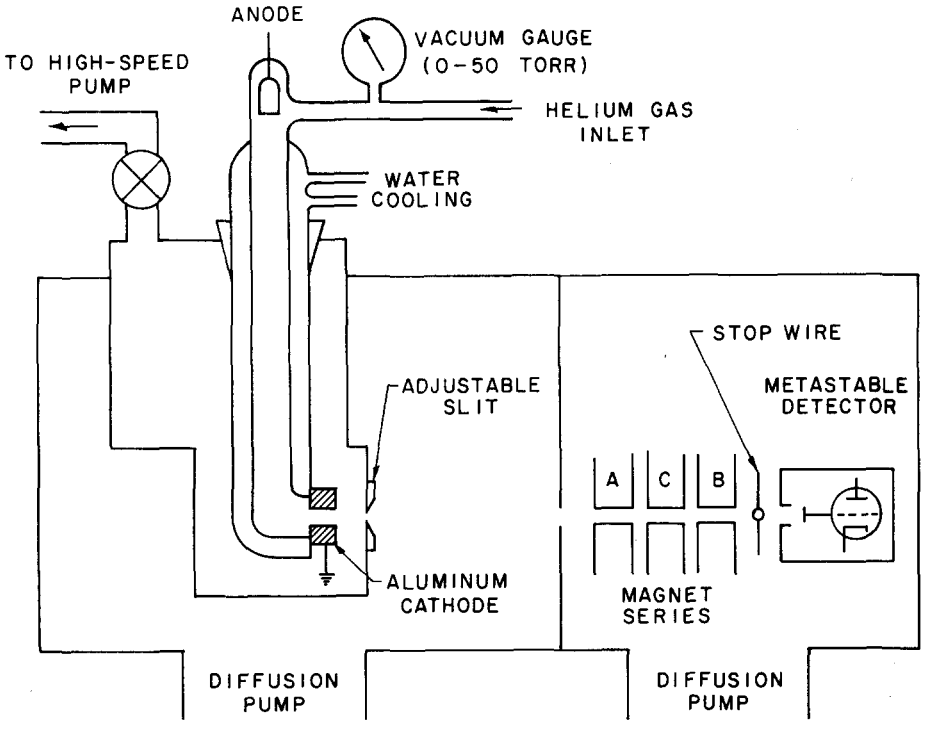

FIG. 3. Apparatus. Schematic view.

C magnet, molecules underwent a transition to a state with a different high field magnetic moment. These molecules were not refocused, and their trajectory allowed them to miss the stop wire and pass into the detector. The pole faces of the three magnets were each 1.908 cm in length, the hairpin was approximately 0.63 cm in length.

The detector consisted of a metal plate connected to the grid of an electrometer tube. Secondary electrons emitted from this plate were collected on a nearby second plate biased to +30 V. The grid bias resistor of the electrometer tube amplifier was 10^{12} Ω, and the time constant of this detector and amplifier was nominally 4 sec.

A block diagram of the data collection system is shown in Fig. 4. The voltage output of the electrometer was read directly on a Hewlett-Packard Model 415A D.C. Null Voltmeter. The output signal from the null voltmeter was recorded on a strip chart recorder as a function of time and also was digitized and recorded in the memory of a PDP-8 computer.

In measuring the line profile of a particular transition, the uniform field in the C magnet was held fixed while the frequency of the oscillating magnetic field was varied under computer control. For the studies of the Zeeman spectrum at low frequencies (see Sec. II. B), the direct output from a General-Radio oscillator was used (Model 1211-C for 0.5-50 MHz, Model 1215-B for 50-250 MHz). For the studies of the fs transitions in the frequency range between 800 and 1200 MHz, the output of a GR oscillator (Model 1209 B, 250-900 MHz) was frequency doubled, and amplified (with an Amptron Model 125 RF amplifier) before entering the C region hairpin. For the transition near 2000 MHz, a klystron oscillator (Applied Microwave Laboratories, Model S-1140), was used directly. Except for the 2 GHz tran-

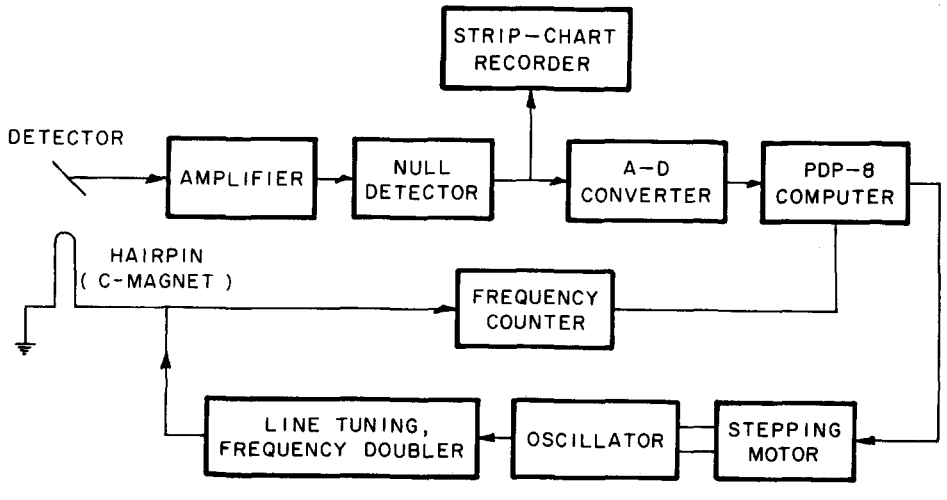

FIG. 4. Electronics. Block diagram.

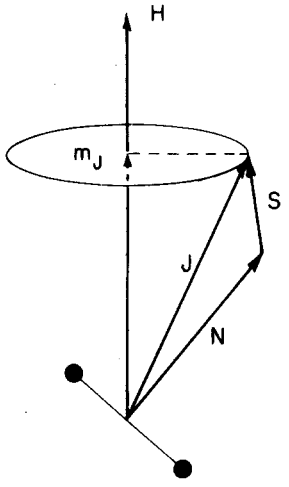

FIG. 5. Vector model for Hund's case *b* coupling in a diatomic molecule in a Σ state, with spin **S**, rotational angular momentum N, total angular momentum J, and magnetic quantum number m_J.

sition, the power line between the oscillator and the hairpin was tuned. This tuning was particularly necessary for the Zeeman studies in order to suppress harmonics of the molecular transition frequencies which would overlap the stronger signal from the metastable 2^3S_1 atoms. The transition frequencies were measured with a calibrated electronic counter (Hewlett-Packard Model 5245 C) with frequency converter plug-in units appropriate to the frequency range being used.

B. Procedure, observations, and data analysis

The field in the *C* region was calibrated with the strong resonance produced by the Zeeman transitions in $He(2^3S_1)$. These transitions had a frequency $f = g_J(\mathrm{He}) \times \mu_0 \mathcal{H}/h$, where $g_J(\mathrm{He}) = 2.00223735(60)$.[62]

The search for $He_2(a^3\Sigma_u^+)$ began with the low-field, Zeeman transitions in the $N = 1$ rotational level. Because He_2 has weak spin-orbit coupling, it follows Hund's case *b* coupling model.[63] In Hund's case *b*, for $^3\Sigma$ states, the rotational angular momentum **N** adds with **S**, the total electronic spin, to form J. The projection of J along the magnetic field direction m_J is quantized. Since He has zero nuclear spin, J represents the total angular momentum of the molecule. (See Fig. 5.) The *g* factor for such a molecule is given by

$$g_J = g_S \frac{J(J+1)+S(S+1)-N(N+1)}{2J(J+1)} + g_N \frac{J(J+1)-S(S+1)+N(N+1)}{2J(J+1)} . \quad (1)$$

In a Σ state, **N** is due to the nuclear rotation and has a corresponding magnetic moment $g_N\mu_0$ of the order of a nuclear magneton, i.e., $g_N \ll g_S$.

If H_0 represents the zero-field Hamiltonian, including electronic, vibrational, rotational, and fine-structure terms, then the Hamiltonian in the *C* field region is

$$H = H_0 - \boldsymbol{\mu} \cdot \boldsymbol{\mathcal{H}} . \quad (2)$$

In order to find the exact eigenenergies at any magnetic field, *H*, a matrix of order $6N+3$ must be diagonalized for each rotational level. (Matrix elements involving states of different *v* or *N* may be neglected; since the perturbation terms contain the unperturbed energy differences in the denominator, effects of these states are at least 3 orders of magnitude less than those due to states in the same vibrational and rotational level.) The diagonal elements expressed in terms of the low-field quantum numbers *N*, *S*, *J*, and m_J are

$$\langle N, S, J, m_J | H | N, S, J, m_J \rangle = E_0(N, S, J) + m_J g_J \mu_0 \mathcal{H} . \quad (3)$$

Off-diagonal elements are nonzero only between states with the same m_J, and are[64]

$$\langle N, S, J, m_J | H | N, S, J-1, m_J \rangle = \left[\frac{(J-N+S)(J+N-S)(J+N+S+1)(N+S+1-J)}{4J^2(2J+1)(2J-1)} (J^2 - m_J^2) \right]^{1/2} (g_S - g_N)\mu_0 \mathcal{H} . \quad (4)$$

Figure 6 shows the results of diagonalization for $N = 3$ as a function of magnetic field. To second order in $\mathcal{H}$, the energy eigenvalues are given by

$$E(N, S, J, m_J) = E_0(N, S, J) + m_J g_J \mu_0 \mathcal{H} + \frac{\langle N, S, J, m_J | H | N, S, J-1, m_J \rangle^2}{E_0(N, S, J) - E_0(N, S, J-1)} + \frac{\langle N, S, J, m_J | H | N, S, J+1, m_J \rangle^2}{E_0(N, S, J) - E_0(N, S, J+1)} . \quad (5)$$

In order for a transition to be observable in this particular MBMR apparatus, the molecule had to undergo a high-field moment change of at least a half Bohr magneton. [The high-field moment is defined as $-(dE/d\mathcal{H})$ at high $\mathcal{H}$.] As the correlation diagram in Fig. 7 illustrates, three of the $N = 1$ Zeeman transitions met this criterion. Since the *g* factors for $J = 1$ and 2 are both very nearly equal to $g_S/2$,[65] these three resonances were predictably found in the vicinity of half the atomic helium frequency. The teletype plotted output of a computer-controlled scan over two of these resonances is shown in Fig. 8. The three observable Zeeman transitions in $N = 3$ were found in a similar manner.

By fitting the observed Zeeman transition frequencies to levels described in Eq. (5) we were able to obtain initial estimates for the fine-structure intervals. These estimates were, in $N = 1$,

$J = 0$ to $J = 1$, 2240 MHz,
$J = 1$ to $J = 2$, 890 MHz. {all ±30 MHz}.

We then used Kramers' formula[30] to estimate the intervals in $N = 3$:

$J = 2$ to $J = 3$, 1350 MHz,
$J = 3$ to $J = 4$, 984 MHz.

This process also enabled us to determine the relative order of the *J* levels within a complete inversion of the

levels.

With these initial estimates, we could predict and begin searching for direct transitions between the fine-structure levels, i.e., $\Delta J = \pm 1$. According to magnetic dipole selection rules, there are $8N-2$ observable transitions between the fine-structure levels of a particular rotational level N; there are 6 in $N=1$ and 22 in $N=3$. Indeed, in a search conducted in the region of our estimates, all $N=1$ and $N=3$ transitions were found. An effort was made to find the $N=5$ transitions, but without decisive results.

For our final experimental evaluation of each fine-structure energy splitting, we measured a selected pair of lines. These were chosen on the basis of large intensity, small C field dependence, and rf power requirements within our capabilities. The C field was kept below 5 G in all final runs so that the energy terms of order higher than $\mathcal{H}^2$ contributed less than 2 kHz to the resonant frequencies. Data taking consisted of scanning the frequency back and forth over each resonance, alternating between lines of a pair, and using the on-line computer signal averaging to obtain the results. Data on each transition were taken on several separate days and at various magnetic fields.

Figure 9 shows a plot of one set of data taken on the $J=2$ to $J=3$ transitions. The magnitude of the signal shown here was typical—2×10^{-16} A at the input of the detector amplifier circuit. The helium atomic resonance was approximately 2×10^{-13} A. If we allow for the greater multiplicity in the molecules and assume equal detection efficiency, this implies an atomic-to-molecular signal ratio of 100 to 1. The molecular signal-to-noise ratio was 2 to 1; a noise analysis of this experiment is summarized in Table I.

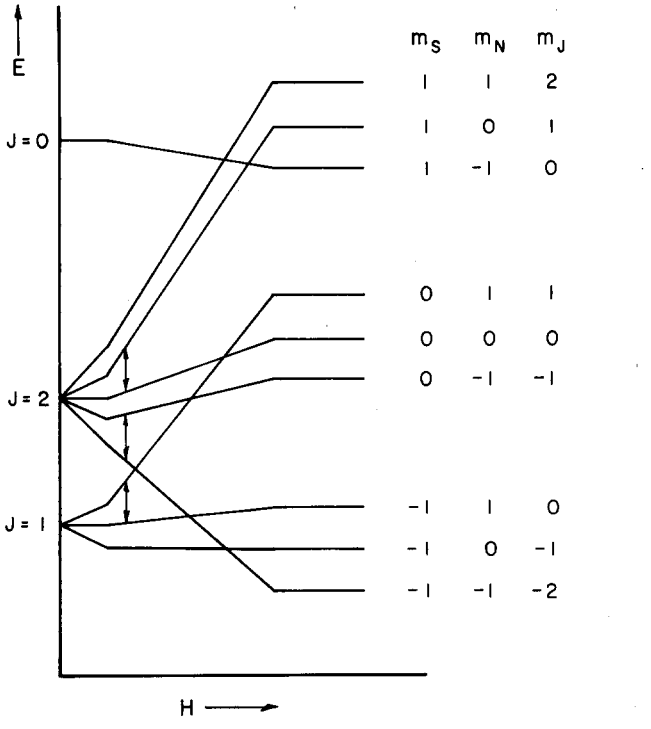

FIG. 7. Correlation diagram for He_2 ($a^3\Sigma_u^+$), $N=1$. Low-field energy levels, where J and m_J are good quantum numbers, are linked with the high-field levels characterized by m_N and m_S in accordance with the noncrossing rule.

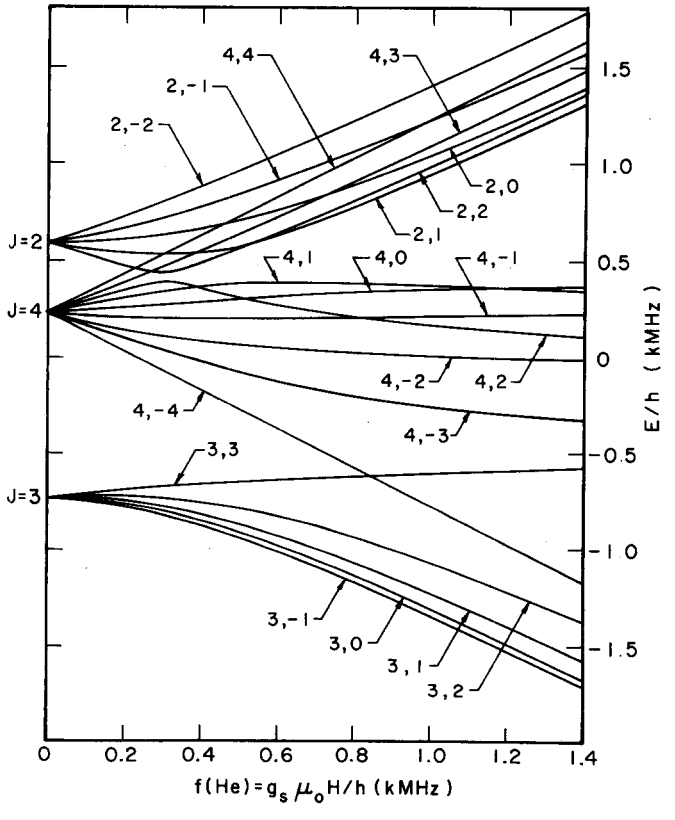

FIG. 6. Energy levels of He_2 ($a^3\Sigma_u^+$), $N=3$ as a function of magnetic field. Levels $(3,-2)$ and $(3,-3)$ have been omitted for clarity.

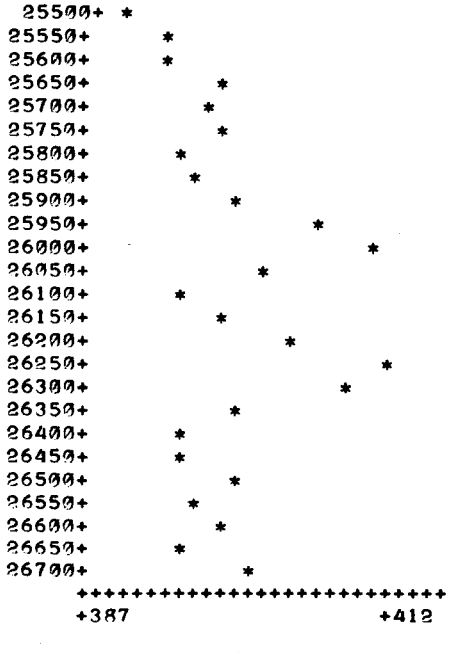

FIG. 8. Graphic computer output of an average of 8 scans over the $(2,-1)\leftrightarrow(2,-2)$ and $(1,1)\leftrightarrow(1,0)$ Zeeman transitions in $N=1$. The atomic helium frequency at this field was 50.49 ± 0.01 MHz.

During the data taking, the rf power was maintained at the level that maximized the transition probability. At this optimum power level, the theoretical linewidth for a v^3 Maxwellian velocity distribution is[66]

$$\Delta f = 1.072\ \alpha/l\ ,$$

where $\alpha = \sqrt{2kT/m}$ and l is the length of the rf region. If all the products of the discharge have nearly the same temperature, and if broadening due to field inhomogeneities is not too large, we may infer that the linewidths of the molecular resonances should have been narrower than the atomic resonances roughly by a factor of $\sqrt{2}$. Typical atomic linewidths of 225–250 kHz would thus imply molecular linewidths of 160–180 kHz. In actuality, the helium molecular resonances ranged from 130–220 kHz in width, but most of the lines were near 160 kHz, in agreement with expectation.[67]

Values for the fine-structure intervals obtained from separate runs were averaged, with weighting factors proportional to the total number of scans per run. The final values are given in Table II.

C. Results. Molecular constants for fs intervals

According to Kramers' theory of spin–spin interaction in diatomic molecules,[30] the energy levels for a $^3\Sigma$ state are given by[68]

$$H = B(N)(N+1) + \tfrac{2}{3}\lambda[3S_Z^2 - \mathbf{S}^2] + \gamma(\mathbf{S}\cdot\mathbf{N})\ , \qquad (6)$$

where $\mathbf{S}$ is the total spin angular momentum, $\mathbf{N}$ is the rotational angular momentum, λ is the spin–spin interaction constant, γ the spin–rotation constant, and B is the rotational constant.

It is readily shown that the resulting term values are (relative to the level with $J = N$)[69]

$$F_1(N) = F(J = N+1) = -\frac{2\lambda(N+1)}{2N+3} + \gamma(N+1)\ ,$$
$$F_2(N) = F(J = N) = 0\ , \qquad (7)$$
$$F_3(N) = F(J = N-1) = -\frac{2\lambda N}{2N-1} - \gamma N\ .$$

Schlapp's formula[31] takes into exact account the perturbation of neighboring rotational levels ($\Delta J = 0$, $\Delta N = \pm 2$) by the spin–spin interaction. It gives the following term values (relative to $J = N$)[70]:

$$F_1(N) = (2N+3)B - \lambda - \sqrt{(2N+3)^2B^2 + \lambda^2 - 2\lambda B} + \gamma(N+1)\ ,$$
$$F_2(N) = 0\ , \qquad (8)$$
$$F_3(N) = -(2N-1)B - \lambda + \sqrt{(2N-1)^2B^2 + \lambda^2 - 2\lambda B} - \gamma N\ .$$

Also, the ambiguity in level order gives two possible sets of constants, which are essentially equal to each other in magnitude, but with opposite sign. Table III gives these two sets, each of which is equally compatible with the experimental data. The uncertainties quoted are obtained by standard error theory from those quoted for the line frequencies.

Since there are four measured intervals in two rotational levels, it was possible to obtain two constants λ and γ for each rotational level. These constants in Table III are given in the form

$$\lambda(N) = \lambda_0 + \lambda_1(N)(N+1)\ ,$$
$$\gamma(N) = \gamma_0 + \gamma_1(N)(N+1)\ , \qquad (9)$$

where λ_0, γ_0 are the magnetic fs constants for a hypothetically nonrotating molecule, and λ_1, γ_1 are centrifugal stretching constants.

TABLE I. Noise sources in a single scan over a molecular resonance. The data are all for single observations with a circuit time constant of 4 sec. All values are in amperes.

Background current	5×10^{-13}
Molecular signal	2×10^{-16}
Estimated thermal noise	3×10^{-17}
Estimated shot noise	8×10^{-17}
Estimated total noise	9×10^{-17}
Observed noise	1×10^{-16}

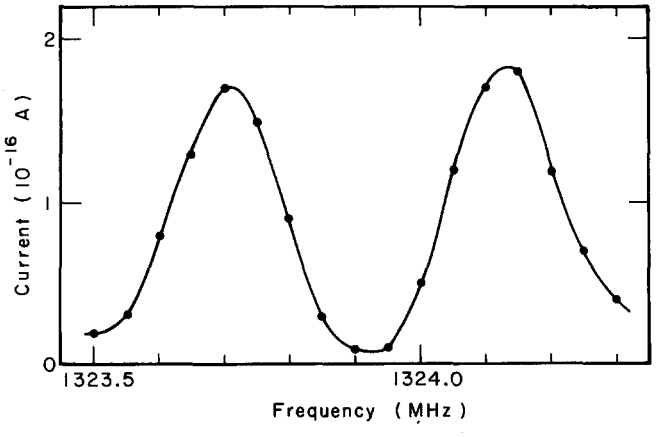

FIG. 9. Results of averaging 20 scans over the transitions $(3,-1)\leftrightarrow(2,0)$ and $(3,1)\leftrightarrow(2,0)$. The atomic helium frequency was 2.54 ± 0.01 MHz; the rf power was 150 mW.

III. DISCUSSION AND INTERPRETATION

A. Identification of spectra

1. *Metastable helium molecules*

As was mentioned in the section on method, every parameter that gave optimal visible molecular helium spectra in the discharge (pressure, electrode polarity, voltage, pulse length and frequency, etc.) also gave a good rf molecular signal. We thus felt that we were indeed looking at metastable helium molecules. For example, the atomic resonances ($^3S_1$, $\Delta m_S = \pm 1$) persisted and even intensified with 100-fold smaller pressures ($\ll 1$ torr) in agreement with the observations of Hughes *et al.*[60] On the other hand, the optimal conditions for observation of the molecular resonances were pressures of the order of 10 torr and a flowing afterglow.

Both the low frequency Zeeman resonances and high frequency lines, which occur only in odd rotational levels, could have come only from homonuclear molecules with zero nuclear spin in a $^3\Sigma_u^+$ or $^3\Sigma_g^-$ state.[71] The only possible impurity that might have given such a spectrum

TABLE II. Fine-structure separations for $N=1$ and $N=3$. Errors are in last place and are three standard deviations (3σ).

N	Interval (J)	Transitions	No. of Scans	Frequency (MHz)
1	$0\leftrightarrow 1$	$(1,-1)\leftrightarrow(0,0)$	56	2199.968 (10)
		$(1,+1)\leftrightarrow(0,0)$	72	
	$1\leftrightarrow 2$	$(2,+2)\leftrightarrow(1,+1)$		
		$(2,+2)\leftrightarrow(1,0)$	75	873.668 (7)
		$(2,0)\leftrightarrow(1,-1)$		
		$(2,-1)\leftrightarrow(1,0)$	84	
3	$2\leftrightarrow 3$	$(3,-1)\leftrightarrow(2,0)$	72	
		$(3,+1)\leftrightarrow(2,0)$	72	1323.911 (6)
	$3\leftrightarrow 4$	$(4,0)\leftrightarrow(3,-1)$	128	
		$(4,+1)\leftrightarrow(3,+2)$		964.992 (6)
		$(4,-1)\leftrightarrow(3,-2)$	128	
		$(4,0)\leftrightarrow(3,+1)$		

is O_2. The $^3\Sigma$ states of this molecule are well known[72] and none has spin–spin constants nearly as small as that of the molecule we have observed. Thus, all the positive evidence and the elimination of alternative possibilities lead to the conclusion that we observed He_2 molecules in the only metastable state, $a^3\Sigma_u^+$.

2. Quantum numbers

The rf spectrum unambiguously fixed the angular momentum quantum numbers (N, S, J) of He_2. The only numbers that were not directly identifiable from our experiment were those of the vibrational levels $v=0$, 1, 2, 3, ...

The presence of two different sets of data ($N=1$ and $N=3$) with spin–spin constants that differ by only a fraction of a percent indicated that all four transitions are in the same vibrational state. If this were not true, discrepancies of the order of a few percent or more would have been caused by variation of the constants with vibrational quantum number.[73]

The resonances between Zeeman sublevels showed no evidence of broadening or splitting, which would have been caused by the detection of more than one vibrational level in the beam. We concluded that we saw molecules in the lowest ($v=0$) vibrational level and that higher states ($v=1, 2, \ldots$) were too weak to be observable.[45,74]

3. Choice of sign of constants

We chose the negative sign for the fs constants λ and γ (see Table III). The reasons for this choice are as follows:

(a) *A priori* estimates. The relative simplicity of the electronic wavefunction dictates that the two electrons tend to interact such that λ is negative. A discussion of this point is given in Paragraph (B) of this section.

(b) *A priori* calculation. A computer calculation of λ from *a priori* molecular wavefunctions by Beck, Nicolaides, and Musher (see Table IV)[75] agreed with the conclusions of paragraph (a) above.

(c) Consistency of constants. The perturbation of the fs by neighboring rotational levels causes a deviation of the true levels from those calculated by Kramers' formula. This shows itself in an inconsistency of the spin-rotation constants (see Table III) between the $N=1$ and $N=3$ levels. These constants for the two levels differ by 4%, an amount that is inconceivably large.

The choice of the positive values for the constants in Schlapp's formula (see Table III) only worsens this effect. The spin-rotation constants for the two rotational levels differ by 8%, an even more inconceivable discrepancy. On the other hand, choice of negative values for λ and γ reduces the discrepancy between spin–rotation constants to 0.3%, an amount which is quite reasonably ascribed to rotational stretching effects. (See Table III and Sec. III.C.)

(d) Direct experimental determination. By placing a set of asymmetric stops in the apparatus, it is possible to measure the sign of the fs intervals directly. Such an experiment is presently underway.[76]

TABLE III. Rotational level constants.

Constant (MHz)	Rotational level $N=1$	Rotational level $N=3$	$N=0$ (extrapolated)	Centrifugal stretching coefficient
Spin–spin (λ)				
From Kramers' formula[a]	± 1098.668 (5)	± 1096.958 (4)	± 1099.010 (5)	∓ 0.1710 (7)
From Schlapp's formula[a]	$+1098.561$ (5)	$+1097.114$ (4)	$+1098.853$ (5)	-0.1448 (7)
	-1098.773 (5)	-1096.803 (4)	-1099.167 (5)	$+0.1970$ (7)
Spin–rotation (γ)				
From Kramers' formula[a]	± 2.633 (3)	± 2.520 (1)	± 2.653 (3)	∓ 0.0113 (3)
From Schlapp's formula[a]	$+2.845$ (3)	$+2.627$ (1)	$+2.885$ (3)	-0.0218 (3)
	-2.421 (3)	-2.414 (1)	-2.422 (3)	$+0.0007$ (3)

[a]There is an ambiguity in the sign of the level spacing. The two values given are obtained from the alternative choice of level order. The value of the rotational constant $B_0=7.6$ cm$^{-1}=228\,000$ MHz was obtained from Ref. 3 (see, also, Ref. 63). Errors are in last place and are three standard deviations.

TABLE IV. Comparison of spin–spin interaction constants λ in several molecules. Units are kaysers (cm^{-1}).[a]

Estimates of λ^{ss} (pure spin–spin part) and λ^{so} (indirect, spin–orbit part)

	λ^{exp}	λ^{ss}_{th}	$\lambda^{so}=\lambda^{exp}-\lambda^{ss}_{th}$	λ^{so}_{th}
$He_2\ ^3\Sigma_u^+$	−0.0367[b]	−0.041[f]		0.000003[i]
$CH_2\ ^3\Sigma^-$		0.454		0.0135 0.0565
$NH\ ^3\Sigma^-$	0.928	0.814	0.114	0.085 0.134
$N_2\ ^3\Sigma_u^+$	1.33[c]			
$O_2\ X\ ^3\Sigma_g^-$	1.985	0.822 0.756[g] 0.708[h]	1.163 1.229 1.277[h]	0.86 0.628[g] 0.871[h]
$B\ ^3\Sigma_u^-$				
$v=0$	1.63[d]	1.14[d]	0.49[d]	
$v=19$	7.63[d]	1.14[d]	6.49[d]	
$SO\ ^3\Sigma^-$	5.276	0.594	4.682	
$S_2\ ^3\Sigma^-$	11.7	0.366	11.3	
$SeO\ ^3\Sigma^-$	84.6	0.5	84.1	
$Se_2\ ^3\Sigma_u^-$	183[e]			
$TeO\ ^3\Sigma^-$	340[e]			

[a]Unless otherwise indicated, all data are taken from K. Kayama and J. C. Baird, J. Chem. Phys. 46, 2604 (1967).
[b]Present measurement.
[c]See Ref. 58.
[d]Obtained from a semiempirical fit to experimental data by T. H. Bergeman and S. C. Wofsy, Chem. Phys. Lett. 15, 104 (1972).
[e]R. F. Barrow and M. R. Hitchings, J. Phys. B 5, L132 (1972).
[f]See Ref. 75.
[g]See Ref. 39.
[h]See Ref. 42.
[i]Order of magnitude estimate by present authors. Arguments given by Beck *et al.* in Ref. 75 indicate that λ^{so}_{th} is much smaller than this value.

B. Interpretation of constants, comparison with simple models and other molecules

The most remarkable aspect of our results is the exceptionally small magnitude of the spin–spin interaction. The absolute value of the spin–spin constant $|\lambda|=1100$ MHz is to be contrasted with values found in other molecules. (See Table IV.) For example, the interaction in He_2 is 50-fold smaller than that in the ground state of O_2.

Note in Table IV that the spin splitting of diatomic Σ states consists of two parts—a direct spin–spin interaction (λ^{ss}) and an indirect, spin–orbit interaction (λ^{so}). The spin–spin term is fairly independent of atomic number and is of the order of 10–20 GHz in Σ^- states formed from two π electrons. Even in H_2, $c^3\Pi_u$, which has one π electron, the spin–spin splitting is of the order of 5 GHz.[19,20] We have seen in Part I. A. 3 that the configuration of $He_2\ a^3\Sigma_u^+$ consists of σ electrons only; $(\sigma_g 1s)^2 \times (\sigma_u 1s)(\sigma_g 2s)$ and the spin–spin interactions arise from the two unpaired electrons $\sigma_u 1s$ and $\sigma_g 2s$.

The spin–spin interaction is zero in the separated atoms: $He_2\ a^3\Sigma_u^+ \rightarrow He(1s)^2\,^1S_0 + He(1s, 2s)^3S_1$; neither atom has any spin splitting. Quantum mechanically, this follows as a result of an angular momentum argument.[77] Classically, the spin–spin interaction in He $^3S_1$ can be viewed as the magnetic influence of two uniformly magnetized spherical shells on each other. Each shell can be viewed as a sphere of north poles slightly displaced from a sphere of south poles of equal magnitude. Outside such a sphere, the field appears to be that of a magnetic dipole, but inside the field is zero. The inner shell is like a dipole in a field free region, with no magnetic energy. Thus, the spin–spin interaction in the $^3S_1$ state of He is zero.

For similar reasons, the magnetic fs in Σ states of He_2 is very small. Consider the unpaired $\sigma_u 1s$ and $\sigma_g 2s$ electrons. The σ_u electron, with its unpaired spin, can be viewed as spending half of its time centered about each of the two He nuclei. (See Fig. 2.) The $\sigma_g 2s$ has two parts. The outer part is nearly spherically symmetric, has its center midway between the two nuclei, and lies largely outside the molecular framework (see Fig. 2). For a hydrogenic 2s orbital, it is readily proven that 95% of the probability density lies in the outer part. By the near spherical symmetry of this outer part, there is no magnetic interaction with the inner $\sigma_u 1s$ electron, as in the $^3S_1$ He atom. The remaining 5% of the $\sigma_g 2s$ wavefunction is found on the inner part of the $\sigma_g 2s$ wavefunction. Since the dimensions of the inner part are small compared to the internuclear separation, the inner $\sigma_g 2s$ electron is centered about each of the two nuclei in a fashion similar to the $\sigma_g 1s$ orbital.

As a rough estimate of the spin–spin interaction, we can take 5% of that for two electrons, one on each of the two He nuclei of He_2. The interaction for two such electrons is $\lambda \approx -15.5$ GHz; for the He_2 molecule, we have 5% of that: $\lambda \approx -0.8$ GHz, in order of magnitude agreement with our experimental result $\lambda = -1100$ MHz.

The interaction in this simple model is opposite in sign to that for $(\pi)^2$, Σ^- states. The explanation for the difference in sign is that σ^2 states tend to have both electrons lying along the internuclear axis, with positive values of the operator $(3\cos^2\theta - 1)$, where[33]

$$\lambda = -3g^2\mu_0(3\cos^2\theta - 1)/8R^3\,,$$

where g is the Landé g factor, μ_0 is the Bohr magneton, R is the length of the vector joining the two electrons, and θ is the angle it makes with the internuclear axis. In π^2, $^3\Sigma^-$ configurations, Tinkham and Strandberg have shown that this operator has a negative sign, as both electrons tend to be across the internuclear axis from each other.[33]

A more precise interpretation awaits computation of the spin–spin operator with an *ab initio* wavefunction. Such calculations are in process.[75] (See Table IV.)

The spin–rotation constant γ cannot be interpreted as simply as the spin–spin constant λ. A simple calculation based on the magnetic field at one nucleus caused by a unit, positive charge at the other nucleus gives a value of $\gamma = +5$ MHz. The observed constant $\gamma = -2.5$ MHz is of this order of magnitude, but further interpretation awaits a detailed calculation.

C. Centrifugal stretching

The calculation of the stretching of the internuclear distance by rotation is elementary and is given in standard references.[78] The change in internuclear distance caused by centrifugal stretching is given by

$$\frac{r-r_e}{r_e}=\frac{4B^2(N)(N+1)}{\omega^2}, \tag{10}$$

where r_e is the equilibrium internuclear distance, B is the rotational constant, and ω is the vibrational constant.[78] If a molecular parameter p scales as the ath power of the internuclear distance, $p \propto r^a$, it can be shown that

$$\frac{d\ln(p)}{d\ln(r)}=a . \tag{11}$$

The values of the power a for the spin–spin and spin–rotation constants of He_2 are given in Table V. For comparison, the same constants are given for molecular oxygen.

If the distances involved in the spin–spin and spin–rotation interactions scaled as the internuclear distance, one would expect a power law of -3 for both parameters. The experimental data for He_2 are in fair agreement with the expectation, but the results for oxygen completely disagree (see Table V).

This is consistent with the picture given in Sec. III. B, where the spins in He_2 interact from separate atoms, while the O_2 spins tend to be on the same atom when contributing to the observed spin–spin fs.

TABLE V. Power law for molecular parameter p, $p \propto r^a$, as derived from centrifugal stretching constant.

Molecule	Interaction	Parameter	Power, a	Reference
He_2	spin–spin	λ	-2.5	a
	spin–rotation	γ	-4.0 ± 1.7	a, d
O_2	spin–spin	λ	$+0.29$	b, c
	spin–rotation	γ	$+0.29$	c

[a]Present experiment.
[b]See Ref. 34.
[c]See Ref. 37.
[d]Error shown is 3σ. Other errors are negligible.

IV. CONCLUSIONS

We have measured the fs of the helium molecule in two different rotational levels. The results are self-consistent and are in reasonable agreement with plausible models. The helium molecule is the most favorable one for comparison of theory and experiment for pure spin–spin interactions. It is very nearly free of the off-diagonal spin–orbit interaction (see Table IV), which has not been handled completely successfully to date by any theoretician,[30–42] in the sense that it has not been completely calculated *ab initio*. He_2 is a four-electron system, with two electrons in a tightly bound, closed shell, which should make relatively accurate calculations possible. The only system of greater simplicity would be H_2, in which there are no measurements at present of fs in $^3\Sigma$ states. Thus, He_2 occupies a unique position in molecular theory.

ACKNOWLEDGMENTS

We are indebted to Richard W. Kadel for valuable assistance in setting up the experiment and taking data. Andrew Patterson, Paul Burrow, George Schulz, Willis Lamb, and William R. Bennett, Jr. kindly lent us equipment. We are especially grateful to A. Patterson for his continued generous help. The Yale Engineering and Applied Science Department was kind enough to allow us use of ample space and the mechanical pump. We acknowledge helpful communications and discussions with Marshall Ginter, Donald Beck, Cleanthis Nicolaides, Richard Alben, and G. King Walters.

APPENDIX A. MOLECULAR HELIUM FORMATION PROCESSES

In our pulsed system, the energy stored in a capacitor is discharged through the source tube in 1 μsec. Electrons are released from the cathode, collide with ground state atoms, and produce excited helium atoms and helium ions (He^*). Molecular ions (He_2^*) are rapidly formed through associative ionization collisions[79] (i.e., collisions between excited helium atoms, with principle quantum number ≥ 3, and ground state atoms)

$$He(n \geq 3)+He \rightarrow He_2^*+e . \tag{A1}$$

We cannot precisely estimate the production rate for this process. The excited state population is rapidly changing with time, particularly in the early afterglow. The rate constant for the reaction

$$He(5^3P)+He \rightarrow He_2^*+e \tag{A2}$$

has been measured[11] to be 8×10^{-11} cm^3/sec at room temperature. This leads to a characteristic reaction time $T=1/k[He]$ (where [He] is the ground state helium) of 3×10^{-6} sec in the afterglow region and 4×10^{-6} sec in the discharge tube. Presumably, the rate constant for other excited states of helium should be similar.

By comparison, the measured rate constant[80,50] for the three-body molecular ion formation

$$He^+ + 2He \rightarrow He_2^* + He \tag{A3}$$

is too small for this process to be significant in our low pressure afterglows.

Similarly, the direct production of the molecules[4]

$$He(2^3S_1)+2He \rightarrow He_2(a^3\Sigma_u^+)+He \tag{A4}$$

is insignificant in our experiment. This process is of importance only in very high pressure systems.

The molecular ions recombine with electrons as they flow through the afterglow region. There is some uncertainty as to the relative probability of dissociative and nondissociative recombination in helium,[52–55] particularly when the molecular ion is in a high vibrational state.[81] In the afterglow where the electron density is high, but after the electron temperature has cooled by elastic collisions with neutrals, the recombination process is collisionally stabilized by a second electron:

$$He_2^+ + 2e \rightarrow He_2^{**} + e \ . \qquad (A5)$$

We cannot measure the electron density in our apparatus. Collins and Robertson,[56] who studied helium flowing afterglows excited by a cw microwave discharge source, observed an electron density of 5×10^{12} cm^{-3} at a time between 50 and 250 μsec into the afterglow. With our pulsed discharge, we anticipate peak electron densities to be at least comparable. If the electron density is assumed to be as low as 10^{12} cm^{-3} at the termination of the discharge pulse, then the recombination rate coefficient[52] is $\alpha \simeq 2\times10^{-8}$ cm^3/sec. This leads to a reaction time of 50 μsec. The recombination rate coefficient in this case is entirely dominated by the electron density, and not by the gas density. The transit time for a molecular ion traveling from the cathode to the exit slit and moving at the bulk flow velocity (see Sec. II. A) is 10 μsec. Within this time, the recombination process can proceed sufficiently to account for the small molecular signals we see (see Table I). We suggest that associative ionization and subsequent electron assisted recombination is a likely molecular production mechanism. This sequence certainly occurs in the lower pressure afterglow; it should also apply to the reactions within the cathode as well as the volume of the discharge tube swept out by the pump between discharge pulses.

*Research supported by the National Science Foundation under Grant NSF GP 27714.

[1]For direct observations of Van der Waals molecules of the rare gases, see Y. Tanaka and K. Yoshino, J. Chem. Phys. 53, 2012 (1970); 57, 2964 (1972). These authors have observed discrete bound states of the HeNe, Ne_2, and Ar_2 molecules. For a recent reference on the potential curve of the ground state of He_2, see J. M. Farrar and Y. T. Lee, J. Chem. Phys. 56, 5801 (1972). The first paper to correctly predict Van der Waals molecules of the rare gases was by D. Ter Haar, W. M. Nicol, and M. P. Barnett, Physica (Utr.) 22, 911 (1956), who concluded there was a bound state in Ne_2. A surprisingly accurate calculation, as confirmed by Tanaka and Yoshino, was done by N. Bernardes and H. Primakoff, J. Chem. Phys. 30, 691 (1959). Since then, there have been a great many references on this subject. See, for example, J. O. Hirschfelder, C. F. Curtiss, and R. B. Bird, *Molecular Theory of Gases and Liquids* (Wiley, New York, 1954), pp. 1064–1075; R. J. Munn, J. Chem. Phys. 40, 1439 (1964); C. T. Chen and R. D. Present, J. Chem. Phys. 54, 3645 (1971); R. D. Etters, J. C. Raich, and P. Chand, J. Chem. Phys. 55, 5130 (1971); R. J. Le Roy, J. Chem. Phys. 57, 573 (1972); D. D. Konowalow and D. S. Zakheim, J. Chem. Phys. 57, 4375 (1972); M. C. Castex and N. Damany, Chem. Phys. Lett. 13, 158 (1972); I. V. Kosinskaya and L. P. Polozova, Opt. Spectrosc. 30, 458 (1971). Clusters of rare gas atoms are well known in nozzle beam experiments. See, for example, T. A. Milne and Frank T. Greene, J. Chem. Phys. 47, 4095 (1967). Chemical compounds of the noble gases were predicted by Pauling in 1933. Recently, many of these have been observed. For a summary and for references, see J. H. Holloway, *Noble-Gas Chemistry* (Methuen, New York, 1968).

[2]W. E. Curtis, Proc. R. Soc. Lond. 89, 146 (1913); E. Goldstein, Verh. Dtsch. Phys. Ges. 11, 402 (1913).

[3]For a summary of the spectra and structure of excited states of He_2, see Marshall L. Ginter, in *Selected Constants, Spectroscopic Data Relative to Diatomic Molecules*, edited by B. Rosen (Pergamon, New York, 1970); M. L. Ginter and R. Battino, J. Chem. Phys. 52, 4469 (1970).

[4]A. V. Phelps, Phys. Rev. 99, 1307 (1955).

[5]A. B. Callear and R. E. M. Hedges, Trans. Faraday Soc. 66, 2921 (1970).

[6]K. H. Ludlum, J. M. Caffrey, and L. P. Larson, J. Opt. Soc. Am. 58, 269 (1968).

[7]J. C. Hill, O. Heybey, and G. K. Walters, Phys. Rev. Lett. 26, 1213 (1971).

[8]J. W. Keto, M. Stockton, and W. A. Fitzsimmons, Phys. Rev. Lett. 28, 792 (1972).

[9]W. A. Fitzsimmons, in *Atomic Physics* 3, edited by S. J. Smith and G. K. Walters (Plenum, New York, 1973), p. 477.

[10]J. Stevefelt and F. Robben, Phys. Rev. A 5, 1502 (1972). These authors use emission, rather than absorption, measurements to estimate molecular concentrations.

[11]C. B. Collins, B. W. Johnson, and M. J. Shaw, J. Chem. Phys. 57, 5310 (1972); C. B. Collins and B. W. Johnson, J. Chem. Phys. 57, 5317 (1972).

[12]G. K. Walters (private communication) states that spin–lattice relaxation in liquid helium is too long to permit observation of resonances in this system.

[13]W. Lichten, Phys. Rev. 126, 1020 (1962).

[14]B. N. Taylor, W. H. Parker, and D. N. Langenberg, Rev. Mod. Phys. 41, 375 (1969). Also published by the same authors as *The Fundamental Constants and Quantum Electrodynamics* (Academic, New York, 1969).

[15]See the reviews by V. W. Hughes (p. 1) and N. M. Kroll (p. 33) in Ref. 9.

[16]J. Daley, M. Douglas, L. Hambro, and N. M. Kroll, Phys. Rev. Lett. 29, 12 (1972).

[17]A. Kponou, V. W. Hughes, C. E. Johnson, S. A. Lewis, and F. M. J. Pichanick, Phys. Rev. Lett. 26, 1613 (1971).

[18]K. B. Jefferts, Phys. Rev. Lett. 23, 1476 (1969); 20, 39 (1968).

[19]A. Dalgarno, T. N. L. Patterson, and W. B. Somerville, Proc. R. Soc. A 259, 100 (1960).

[20]S. K. Luke, Astrophys. J. 156, 761 (1969).

[21]P. R. Brooks, W. Lichten, and R. Reno, Phys. Rev. A 4, 2217 (1971).

[22]W. Lichten and T. L. Vierima (unpublished results). In the latter experiment, we have made vibrational assignments of the p–H_2 transitions.

[23]For references, see W. Lichten, Phys. Rev. A 3, 594 (1971).

[24]T. A. Miller and R. S. Freund, J. Chem. Phys. 56, 3165 (1972); 58, 2345 (1973).

[25]R. S. Freund and T. A. Miller, J. Chem. Phys. 58, 3565 (1973).

[26]M. Lombardi, J. Chem. Phys. 58, 797 (1973).

[27]N. Jette (private communication).

[28]R. S. Mulliken and G. Monk, Phys. Rev. 34, 1530 (1929).

[29]W. Lichten (unpublished experiments). The author wishes to thank Henry Stroke, then at M.I.T., and Mark Fred of Argonne National Laboratory for their kindness in allowing the use of their high resolution equipment for these experiments.

[30]H. A. Kramers, Z. Phys. 53, 422 (1929).

[31]R. Schlapp, Phys. Rev. 51, 342 (1937).

[32]M. H. Hebb, Phys. Rev. 49, 610 (1936).

[33]M. Tinkham and M.W. P. Strandberg, Phys. Rev. 97, 937 (1955); 97, 951 (1955).

[34]S. L. Miller and C. H. Townes, Phys. Rev. 90, 537 (1953).

[35]I. Kovács, Phys. Rev. 128, 663 (1962); see also I. Kovács, *Rotational Structure in the Spectra of Diatomic Molecules*, (American Elsevier, New York, 1969), pp. 72ff.

[36]K. Kayama, J. Chem. Phys. 42, 622 (1965); K. Kayama and J. C. Baird, J. Chem. Phys. 43, 1082 (1965); 46, 2604 (1967).

[37]K. M. Evenson and M. Mizushima, Phys. Rev. A 6, 2197 (1972); W. M. Welch and M. Mizushima, Phys. Rev. A 5, 2692 (1972).

[38]O. Zamani-Khamiri and H. F. Hameka, J. Chem. Phys. 55, 2191 (1971).

[39]R. H. Pritchard, C. W. Kern, O. Zamani-Khamiri, and H. F. Hameka, J. Chem. Phys. **56**, 5744 (1972).
[40]L. Veseth, J. Phys. B **5**, 229 (1972).
[41]T. J. Cook, B. R. Zegarski, W. H. Breckenridge, and T. A. Miller, J. Chem. Phys. **58**, 1548 (1973).
[42](a) R. H. Pritchard, M. L. Sink, J. D. Allen, and C. W. Kern, Chem. Phys. Lett. **17**, 157 (1972); (b) J. A. Lounsbury, J. Chem. Phys. **42**, 1549 (1965).
[43]A. E. Douglas and G. Herzberg, Phys. Rev. **76**, 1529 (1949).
[44]R. A. Buckingham and A. Dalgarno, Proc. R. Soc. Lond. A **213**, 327, 506 (1952), first predicted a small hump in the $a^3\Sigma_u^+$ and $A^1\Sigma_u^+$ states. Mulliken predicted large humps in many other states of He_2 in Phys. Rev. **136**, A962 (1964). Evidence for the maximum in the $a^3\Sigma_u^+$ state comes from optical pumping experiments of F. D. Colegrove, L. D. Schearer, and G. K. Walters, Phys. Rev. **132**, 2561 (1963); W. A. Fitzsimmons, N. F. Lane, and G. K. Walters, Phys. Rev. **174**, 193 (1968). Vacuum ultraviolet emission and absorption experiments support the hump in the $^1\Sigma_u^+$ state: J. L. Nickerson, Phys. Rev. **47**, 707 (1935); Y. Tanaka and K. Yoshino, J. Chem. Phys. **39**, 3081 (1963); **50**, 3087 (1969). For a summary of the experimental data on potential energy curves of He_2, see Ref. 3, also M. L. Ginter and C. M. Brown, J. Chem. Phys. **56**, 672 (1972). For additional calculations of potential curves, see J. C. Browne, J. Chem. Phys. **42**, 2826 (1965), also J. C. Browne and F. A. Matsen, Adv. Chem. Phys. **23**, 161 (1973). G. H. Brigman, S. J. Brient, and F. A. Matsen, J. Chem. Phys. **34**, 958 (1961); R. D. Poshusta and F. A. Matsen, Phys. Rev. **132**, 307 (1963); D. J. Klein, E. M. Greenawalt, and F. A. Matsen, J. Chem. Phys. **47**, 4820 (1967); B. K. Gupta and F. A. Matsen, J. Chem. Phys. **47**, 4860 (1967); **50**, 3797 (1969); F. A. Matsen and D. R. Scott, *Quantum Theory of Atoms, Molecules and the Solid State*, edited by P. O. Löwdin (Academic, New York, 1966); B. Liu, Phys. Rev. Lett. **27**, 1251 (1971); S. L. Guberman and W. A. Goddard III, Chem. Phys. Lett. **14**, 460 (1972); B. K. Gupta, Mol. Phys. **23**, 75 (1972); K. M. Sando and A. Dalgarno, Mol. Phys. **20**, 103 (1971).
[45]W. Weizel and C. Füchtbauer, Z. Phys. **44**, 431 (1927) found that the 0–1 bands of the $2s-3p$ transitions were approximately 10–20 times weaker than the 0–0 bands. Likewise, Ginter (private communication) estimates the 1–0 bands to be 5–10 times weaker than the 0–0 bands. Both of these observations indicate that the radiative formation of the $v=1$ level of the metastable $2s\sigma\ ^3\Sigma_u^+$ state is about five times smaller than the $v=0$ level. (Formation of vibrational levels higher than $v=1$ is much weaker.) This is confirmed by direct observation by Callear and Hedges (see Ref. 5) of absorption by metastable He_2 molecules in the $a\ ^3\Sigma_u^+$ state in the afterglow of a pulsed discharge. These investigators found an initial value of 0.3 for the ratio of $(v=1)/(v=0)$ populations, with fast relaxation to the lowest vibrational state for high pressures.
[46]D. Smith and M. J. Copsey, J. Phys. B **1**, 650 (1968).
[47]A. L. Schmeltekopf and H. P. Broida, J. Chem. Phys. **39**, 1261 (1963).
[48]D. K. Bohme, N. G. Adams, M. Mosesman, D. B. Dunkin, and E. E. Ferguson, J. Chem. Phys. **52**, 5094 (1970).
[49]A. V. Phelps and J. P. Molnar, Phys. Rev. **89**, 1202 (1953).
[50]H. J. Oskam and V. R. Mittelstadt, Phys. Rev. **132**, 1445 (1963).
[51]D. C. Lorents and R. E. Olson, S.R.I. Semi-Annual Technical Report No. 1, ONR Contract N00014-72-c-0457, December 1972 (unpublished).
[52]J. Berlande, M. Cheret, R. Deloche, A. Gonfalone, and C. Manus, Phys. Rev. A **1**, 887 (1970).
[53]A. W. Johnson and J. B. Gerardo, Phys. Rev. A **7**, 925 (1973); Phys. Rev. Lett. **28**, 1096 (1972).
[54]E. E. Ferguson, F. C. Fehsenfeld, and A. L. Schmeltekopf, Phys. Rev. **138**, A381 (1965).
[55]J. N. Bardsley and M. A. Biondi, Adv. At. Mol. Phys. **6**, 4 (1970).
[56]It is known that the electrons in an optically pumped helium afterglow are polarized [M. V. McCusker, L. L. Hatfield, and G. K. Walters, Phys. Rev. A **5**, 177 (1972); P. Keliher, M. O'Neill, M. V. McCusker, R. Rundel, and G. K. Walters, Bull. Am. Phys. Soc. **16**, 1341 (1971)]. The observation of molecular emission bands that populate the $a\ ^3\Sigma_u^+$ state in the afterglow of a microwave discharge in pure helium [See Ref. 45 and C. B. Collins and W. W. Robertson, J. Chem. Phys. **40**, 2208 (1964)] and the development of spin-exchange optical pumping techniques by Schearer [L. D. Schearer, Phys. Lett. A **31**, 457 (1970)], suggest that polarized helium molecules might be produced in an afterglow under some source conditions. Despite the appeal of this approach, it is not obvious that the particular conditions for polarizing molecules can easily be met.
[57]H. A. Koehler, L. J. Ferderber, D. L. Redhead, and P. J. Ebert, Phys. Rev. A **9**, 768 (1974).
[58]D. De Santis, A. Lurio, T. A. Miller, and R. S. Freund, J. Chem. Phys. **53**, 2290 (1970); **58**, 4625 (1973).
[59]G. H. Dieke and E. S. Robinson, Phys. Rev. **80**, 1 (1950).
[60]V. W. Hughes, G. Tucker, E. Rhoderick, and G. Weinreich, Phys. Rev. **91**, 828 (1953).
[61]The cathode hole was initially aligned with the center of the exit slit; the optimum signal-to-noise ratio was obtained when the discharge tube was rotated and translated rather far from this position of geometrical alignment. The background signal is primarily caused by uv photons that are created in the discharge and the early afterglow. This background is maximized when the cathode axis is aligned with the slit, and has a bell shaped distribution curve with respect to sideways translation of the source. The molecular signal, however, is not maximum in the directly aligned position but, rather, has a pronounced minimum there. The position for maximum signal was found in the wings of the background distribution. Thus, the optimum signal-to-noise ratio was found in the wings of the photon background. We are unable to explain these results.
[62]E. Aygün, B. Zak, and H. Shugart, Phys. Rev. Lett. **31**, 803 (1973).
[63]G. Herzberg, *Spectra of Diatomic Molecules* (Van Nostrand-Reinhold, New York, 1950) 2nd ed., p. 221.
[64]See, for example, E. U. Condon and G. H. Shortley, *The Theory of Atomic Spectra* (Cambridge U. P., New York, 1967), p. 391.
[65]Our measured g_J value for $N=1$, $J=1,2$ was $(0.99994 \pm 0.00014)\ g_J(\mathrm{He})/2$, and for $N=3$, $J=4$ was $(0.99940 \pm 0.00004)\ g_J(\mathrm{He})/4$, where the quoted error is one standard deviation. This is in good agreement with our assumption that $g_J(He_2) \sim g_S(\mathrm{He})$ and $g_N \sim 0$.
[66]N. F. Ramsey, *Molecular Beams* (Oxford U. P., New York, 1956), pp. 123–4.
[67]The variation in linewidths can be partly understood in accordance with what one would expect from the state dependent velocity selection in this apparatus.
[68]See Ref. 33, Eq. (5), p. 938.
[69]See Ref. 63, Formula (V, 18), p. 223.
[70]See Ref. 63, Formula (V, 17), p. 223.
[71]The conclusion that the molecule is in a $^3\Sigma$ state and must consist of two identical, spinless nuclei follows from the Zeeman pattern of the rf transitions. The symmetry of the rotational levels determines the character of the electronic wavefunction. See Ref. 63.
[72]Reference 3, see Table I and Ref. 63. N_2, another common impurity, has nuclear spin. The well known Zeeman structure of metastable N_2, observed by Freund *et al.* (Ref. 58) is completely different from our spectrum. Also, in He discharges, only ionized spectra of impurities are found to predominate over the neutral species. The only conceivable molecular impurity that could exist in neutral form in a helium discharge would be NeHe or Ne_2. Formation of such molecules is wholly unlikely at the low impurity levels in commerical tank helium.

[73]Discrepancies of the order of several percent were found in the rf spectra of metastable hydrogen molecules, but have recently been resolved by the discovery of transitions in more than one vibrational level and a recent calculation of the spin-rotation constant by Jette. (See Refs. 21, 22, and 27.)

[74]In the afterglow of our fast-flow system, we have not reproduced the high pressure conditions of most optical spectroscopists (see Ref. 45); the collisional relaxation processes could be slow compared to the transport time through the afterglow. However, Schmeltekopf and Broida (Ref. 47) observed 465.0 nm band emission in a flowing afterglow system similar to ours, but at somewhat later afterglow times. The radiation at this wavelength corresponds to the 0–0 transition of the $e^3\Pi_g - a^3\Sigma_u^+$ system. The 1–1 band would have peak intensity at 467 nm. At this wavelength, their published spectra show no emission that is not part of the 0–0 band. Thus, we conclude that we are observing molecules in the $v = 0$ state also.

[75]D. Beck, C. Nicolaides, and J. Musher (unpublished results).

[76]For a description of procedure and results of the determination, see T. L. Vierima, Ph.D. thesis, Yale University, 1974. Since this manuscript was written, these measurements have been completed and confirm our choice of the sign of the constants. The results of this auxiliary experiment will be submitted by T. L. Vierima to the Comments section of J. Chem. Phys.

[77]H. A. Bethe and E. E. Salpeter, *Quantum Mechanics of One- and Two-Electron Atoms* (Academic, New York, 1957), pp. 186–7.

[78]See Ref. 63, p. 103.

[79]J. A. Hornbeck and J. P. Molnar, Phys. Rev. **84**, 621 (1951).

[80]E. C. Beaty and P. Patterson, Phys. Rev. **137**, A346 (1965).

[81]R. S. Mulliken (see Ref. 44).